Electronic Supplementary Information for

Modification of a pyrene group makes a Ru(II) complex versatile

Zhihui Jin,[ab] Shuang Qi,[ab] Xusheng Guo,[ab] Yao Jian,[ab] Yuanjun Hou,[a] Chao Li,[a] Xuesong Wang,*[ab] Qianxiong Zhou*[a]

[a] *Key Laboratory of Photochemical Conversion and Optoelectronic Materials, Technical Institute of Physics and Chemistry, Chinese Academy of Sciences, Beijing 100190, P. R. China. Fax: +86-10-62564049; Tel: +86-10-82543592;*

[b] *University of Chinese Academy of Sciences, Beijing 100049, P. R. China.*

E-mail: xswang@mail.ipc.ac.cn (X.Wang); zhouqianxiong@mail.ipc.ac.cn (Q. Zhou).

Experimental section

Materials

1-Pyrenecarboxaldehyde, 2-acetylpyridine, $RuCl_3 \cdot nH_2O$, 4,7-diphenyl-1,10-phenanthroline, 2,2':6',2"-terpyridine and 1,3-diphenylisobenzofuran were purchased from Sigma Aldrich. 30% ammonia solution and sodium hydroxide were purchased from Innochem. Annexin V-FITC/PI apoptosis detection kit and Calcein-AM/PI live/dead cell double staining kit were purchased from Solarbio. Dulbecco's modification of Eagle's medium (DMEM), penicillin, streptomycin, and fetal bovine serum were purchased from Corning.

Instruments

^1H NMR spectra were recorded on a Bruker DMX-400 MHz spectrometer. ESI mass spectrometry (ESI-MS) spectra were obtained on a Brucker APEX IV (7.0T) FT_MS. UV-vis absorption spectra were measured on a Shimadzu UV-1601 spectrophotometer.

An LED lamp (470 ± 10 nm) was used as the light source for one-photon assays. Spitfire PRO-F1KXP femtosecond amplified laser (800 nm) was used as the light source for two-photon assays.

Nanosecond transient absorption measurements were performed on a LP-980KS laser flash photolysis setup (Edinburgh). Excitation at 450 nm with a power of 2.0 mJ $pulse^{-1}$ from a computer-controlled Nd:YAG laser/OPO system from Opotek (Spectra Physics) operating at 10 Hz was directed to the sample with an optical absorbance of 0.3 at the excitation wavelength. The laser and analyzing light beam passed perpendicularly through a 1 cm quartz cell. The complete time-resolved spectra were obtained using a gated CCD camera (AndoriSTAR); the kinetic traces were detected by a Tektronix MDO 3022 oscilloscope and a R928P photomultiplier and analyzed by Edinburgh analytical software (LP980KS). All samples used in the flash photolysis experiments were deaerated for 30 min with argon before measurements.

Laser confocal scanning microscope images were collected on an Olympus FV1000.

ICP-MS was tested on a PerkinElmer ELAN DRC-e. Measurements were acquired in KED or kinetic energy discrimination mode at 1200 W plasma RF power and 3 V KED voltage. The nebulizer, auxiliary, and collision gas flow rates were 15, 0.7, and 1.0 L/min, respectively. Ru was the target isotope monitored. Calibration curves were obtained along with each run on the ICP-MS using the Ru standard from Sigma-Aldrich.

HPLC analysis was performed on a Vanquish UHPLC series instrument using a WH-C-18 column (5 μm, 4 mm × 150 mm) under the following conditions: detection at 360 nm, 0.1 mL/min flow rate with 95% CH_3CN and 5% H_2O (containing 0.5% formic acid) for complex **1** or 97% CH_3CN and 3% H_2O (containing 0.1% formic acid) for complex **2** in 10 min.

Methods

DFT theoretical calculations

All calculations were carried out with the Gaussian 09 (G09) program package 3,[S1] using the density functional theory (DFT) method with Becke's three-parameter hybrid functional and LeeYang-Parr's gradient corrected correlation functional (B3LYP).[S2] The LANL2DZ basis set and effective core potential were used for the Ru atom, [S3] and the 6-31 G** basis set was used for other atoms.[S4] The ground-state geometry of the complex was optimized in CH_3CN using the conductive polarizable continuum model (CPCM), and frequency calculation was performed to verify that the optimized structure was in an energy minimum state.

MTT assay

Cells are seeded on 96-well plates at a density of 5000-8000 per well and cultured for 24 h. Then complexes 1 or 2 (mother liquor with a concentration of 10 mM in DMSO), or cisplatin (mother

liquor with a concentration of 5 mM in H_2O) was diluted in serum-free DMEM with various concentrations. After incubation for 4 h, the medium was changed. The light groups were illuminated with LED lamp (470 ± 10 nm, 22.5 mW/cm^2) for 30 min, and the cells were incubated for another 24 h. A similar procedure except for light irradiation was carried out for the dark groups. After that, DMEM medium was discarded and MTT (3-(4,5-dimethyl-2-thiazolyl)-2,5-diphenyl tetrazolium bromide) (1 mg/mL) was added. After 4 h, the culture medium was discarded and DMSO/CH_3OH (1:1) was added. The data were obtained by a Thermo MK3 Multiscan microplate reader at 570 nm.

Cell Culture in hypoxia

A549 cells were cultured in DMEM containing 10% FBS, with 3% O_2 and 5% CO_2 (N_2 was another gas source to control O_2 partial pressure).

Apoptosis assay

Annexin V-FITC and PI are double staining reagents for detecting apoptosis and necrosis. A549 cells were co-cultured with complexes for 4 h, and the light groups were irradiated with LED lamp (470 ± 10 nm, 22.5 mW/cm^2) for 30 min. After continual culture for another 10 h, the cells were trypsinized, centrifuged and washed with PBS for 3 times, then were stained with Annexin V-FITC and PI, and analyzed by flow cytometry.

Singlet oxygen quantum yield measurement

The singlet oxygen quantum yield (Φ) was measured according to a reported method,[S5] using 1,3-diphenylisobenzofuran (DPBF) as the singlet oxygen trap, and $[Ru(bpy)_3]^{2+}$ (Φ = 0.81 in CH_3OH) as a reference. The sample was irradiated with 450 nm light source in a Hitachi F-4600 fluorescence spectrophotometer (slit width: 10 nm). The relative singlet oxygen quantum yield is calculated by the following formula:

$$\frac{-\Delta[DPBF]}{t} = \frac{I_0 - I_t}{t} = I_{in}\varphi_{ab}\varphi_{\Delta}\varphi_{\gamma}$$

$$\frac{k}{ks} = \frac{\varphi_{ab}\varphi_{\Delta}}{\varphi^s{}_{ab}\varphi^s{}_{\Delta}}$$

in which t stands for irradiation time; Φ_{ab}, Φ_{γ}, Φ_{Δ} stand for the light absorption efficiency of the photosensitizer, the reaction efficiency of DPBF and $^1O_2$, and the singlet oxygen quantum yield, respectively; I_{in}, I_0 and I_t are incident light intensity, DPBF fluorescence intensity before and after illumination, respectively. K represents the slope of attenuation line of DPBF fluorescence intensity over irradiation time.

Oil(n-octanol)/water partition coefficient (log *P*o/w) measurement

A small amount of complex was added into 3 mL *n*-octanol and 3 mL H_2O. The mixture was sonicated for 20 min, and then centrifuged for 10 min. The absorbance in the two phases was measured separately. The oil/water partition coefficients were calculated using the equation: log*P* = log (A_O/A_W), where A_O and A_W represent the absorption values of the complex in *n*-octanol and in H_2O, respectively.

Cellular uptake

A549 cells were cultured in a 25 cm^2 culture flask for 24 h. The examined complex (1 μL of the 10 mM mother liquor in DMSO was added to obtain a final concentration of 1 μM) was added,

and cultured for 4 h. The A549 cells were digested with trypsin, and collected with centrifugation after being washed three times with PBS. The uptake level was examined using inductively coupled plasma mass spectrometry (ICP-MS) by measurement of the Ru content.

Assay for the lysosomal membrane permeabilization (Acridine Orange assay).

The A549 cells were co-cultured with complex for 4 h, then irradiated with 470 nm LED light for 30 min, placed in an incubator for another 8 h. Then A549 cells were cultured for 20 min with a medium containing 0.5 μM acridine orange. Washed three times with PBS, culture medium was added, and images were collected with confocal microscope.

Cell morphological change upon two-photon irradiation

A549 cells were co-cultured with the compound for 4 h, then the culture medium was refreshed. The morphology of A549 cells upon two-photon irradiation were investigated using confocal microscope (light source: the two-photon femtosecond laser (740 nm, 1.9 W/cm^2) equipped in the microscope).

Cytotoxicity against 3D multicellular spheroids (MCSs)

5000~8000 A549/Cis cells were seeded in a 96-well plate to form MCSs with diameters of about 600 μm. The MCSs were co-cultured with complexes **1** or **2** for 4 h, then the medium was changed to fresh one. The light group was irradiated with a femtosecond laser (800 nm 1 W/cm^2) for 20 min, then was incubated for another 24 h. After that, the MCSs were stained with Calcein-AM and PI for 1 h, and were investigated with a confocal microscope (excited with 488 nm and 561 nm).

Synthesis

The tpy-Py ligand[S6] and $[Ru(dip)_2Cl_2]$[S7] was synthesized following the reported methods.

Synthesis and characterization of $[Ru(dip)_2(tpy\text{-}Py)]^{2+}$ (complex 1)

50 mg $[Ru(dip)_2Cl_2]$ (0.0598 mmol) and 26 mg tpy-Py (0.0598 mmol) were refluxed in methanol/H_2O (7:1) under an argon atmosphere for 10 h. After cooling to room temperature, the mixture was filtered and the solvent was removed by rotary evaporator. The crude product was purified by column chromatography using CH_3CN/saturated KNO_3 aqueous solution (5:1) as the eluent. The purified compound was dissolved in CH_3OH, and NH_4PF_6 was added to get the red precipitates. Yield: 75%. HPLC purity＞95%. ^{1}H NMR (400 MHz, CD_3CN) δ 6.46-6.69 (s, 2H), 6.91-7.00 (d, *J* = 5.6 Hz, 2H), 7.08-7.16 (t, *J* = 8.1 Hz, 1H), 7.28-7.43 (m, 3H), 7.46-7.81 (m, 21H), 7.85-7.90 (d, *J* = 5.4 Hz, 1H), 8.00-8.62 (m, 18H), 8.73-8.81 (d, *J* = 8.3 Hz, 1H), 8.99-9.05 (s, 1H), 9.40-9.56 (s, 1H). ^{13}C NMR (101 MHz, CD_3CN, the peaks cannot be well resolved due to overlapping) δ 165.41, 159.11, 157.11, 155.93, 153.07, 152.76, 152.70, 152.65, 151.48, 149.94, 149.85, 149.50, 149.20, 149.01, 148.32, 147.67, 138.54, 136.98, 136.68, 136.33, 136.28, 132.94, 132.65, 132.05, 131.45, 130.95, 130.70, 130.67, 130.47, 130.40, 130.34, 130.23, 129.91, 129.83, 129.78, 129.70, 129.58, 129.46, 128.95, 128.61, 128.32, 128.00, 127.94, 127.53, 126.96, 126.92, 126.80, 126.74, 126.64, 126.52, 126.49, 126.44, 126.24, 126.05, 125.94, 125.80, 125.28, 124.92, 124.67, 124.47, 123.57. HR ESI-MS: calculated m/z for $(M\text{-}2PF_6^-)^{2+}$: 599.6625, found: 599.6623. Elemental analysis: Calculated for $[C_{79}H_{51}N_7Ru]$ $(PF_6)_2$: (C, 63.71; H, 3.45; N, 6.58). Found: (C, 63.83; H, 3.42; N, 6.69).

Synthesis and characterization of $[Ru(dip)_2(tpy)]^{2+}$ (complex 2)

Complex **2** was synthesized with a procedure similar to that of **1**. Yield: 86%. HPLC purity＞95%.^{1}H NMR (400 MHz, CD_3CN) 6.91-7.01 (d, *J* = 5.7 Hz, 3H), 7.06-7.17 (s, 1H), 7.23-8.40 (m,

34H), 8.67-8.80 (t, J = 9.6 Hz, 2H), 9.06-9.35 (s, 3H). ^{13}C NMR (101 MHz, CD_3CN, the peaks cannot be well resolved due to overlapping) δ 165.52, 159.04, 158.89, 157.04, 155.61, 152.98, 152.66, 152.55, 149.86, 149.77, 149.74, 149.44, 149.39, 149.11, 148.92, 148.19, 147.59, 139.05, 138.59, 136.86, 136.62, 136.30, 136.25, 130.64, 130.61, 130.44, 130.35, 130.31, 130.19, 129.86, 129.84, 129.80, 129.73, 129.60, 129.53, 128.54, 127.87, 126.89, 126.78, 126.63, 126.53, 126.45, 126.39, 126.18, 125.81, 124.53, 123.29. HR ESI-MS: Calculated m/z for $(M\text{-}2PF_6^-)^{2+}$: 499.6312, found: 499.6296. Elemental analysis: Calculated for $[C_{79}H_{51}N_7Ru]$ $(PF_6)_2$: (C, 58.70; H, 3.36; N, 7.61). Found: (C, 58.61; H, 3.41; N, 7.75).

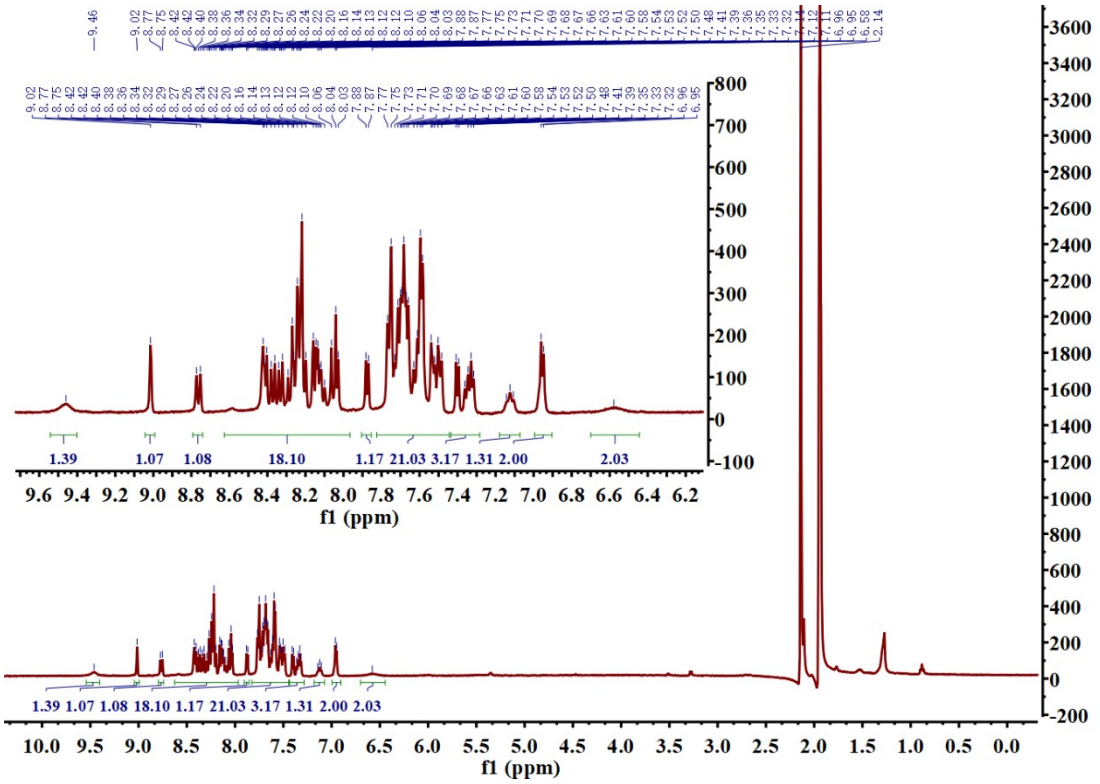

Fig. S1 ^{1}H NMR spectrum of complex **1** in CD_3CN.

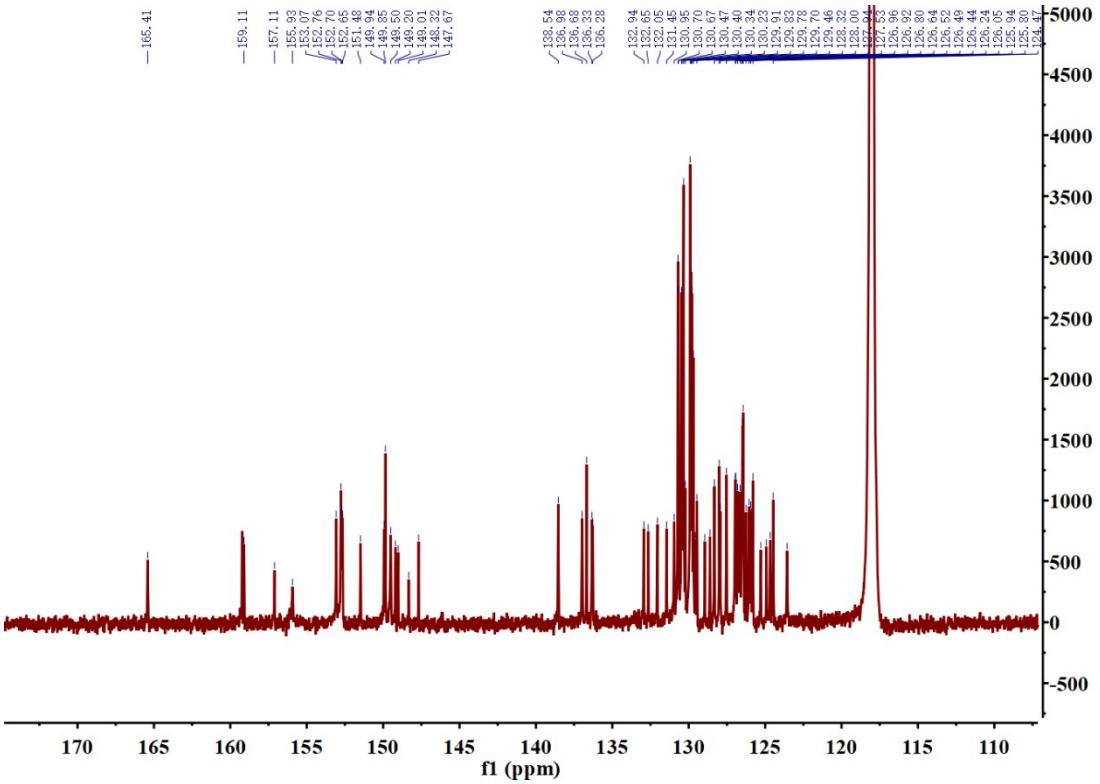

Fig. S2 ^{13}C NMR spectrum of complex **1** in CD_3CN.

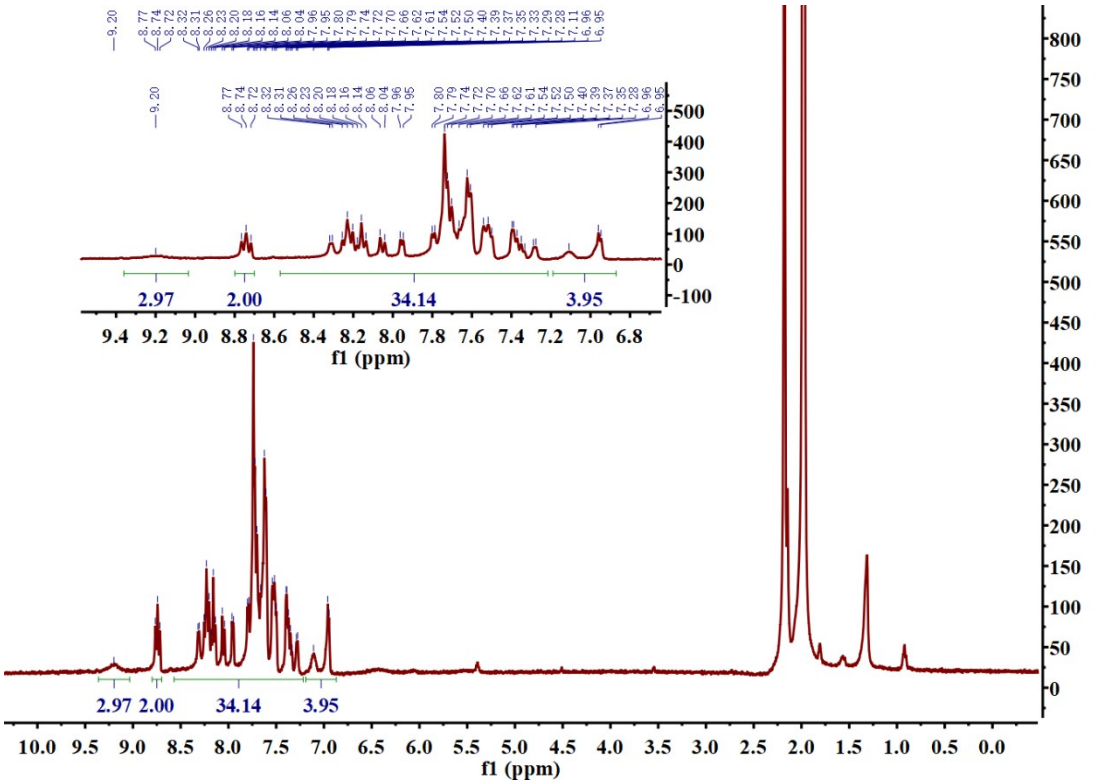

Fig. S3 ^{1}H NMR spectrum of complex **2** in CD_3CN.

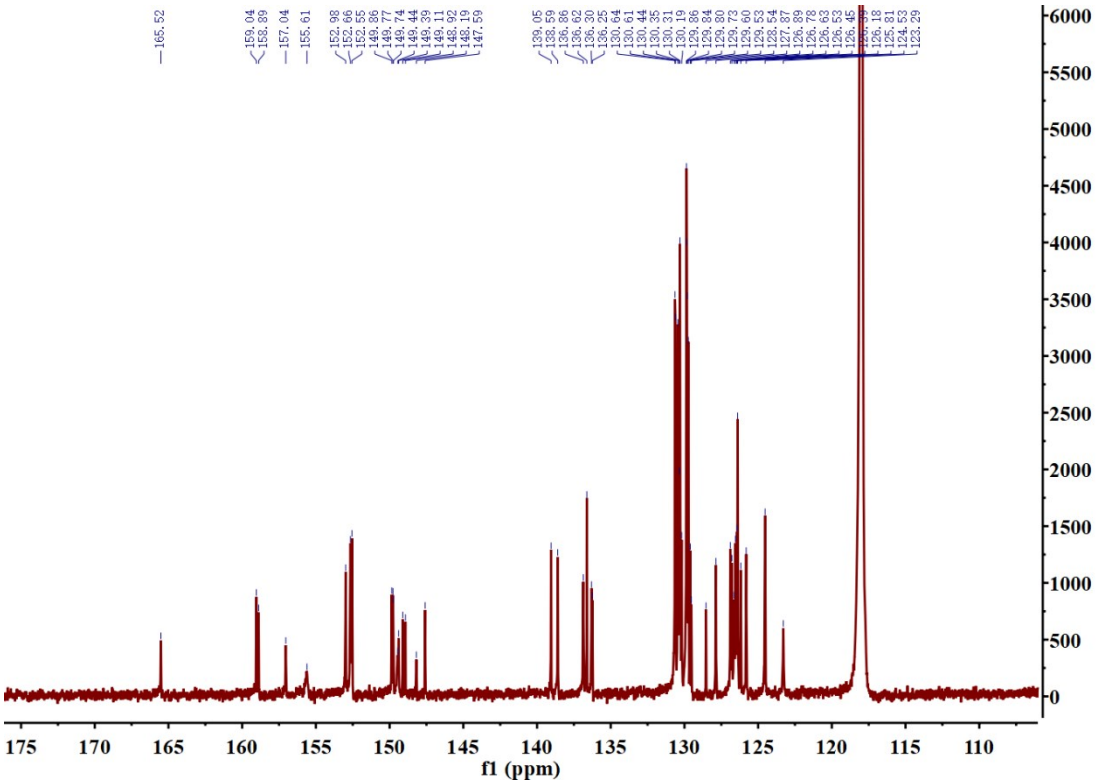

Fig. S4 ^{13}C NMR spectrum of complex **2** in CD_3CN.

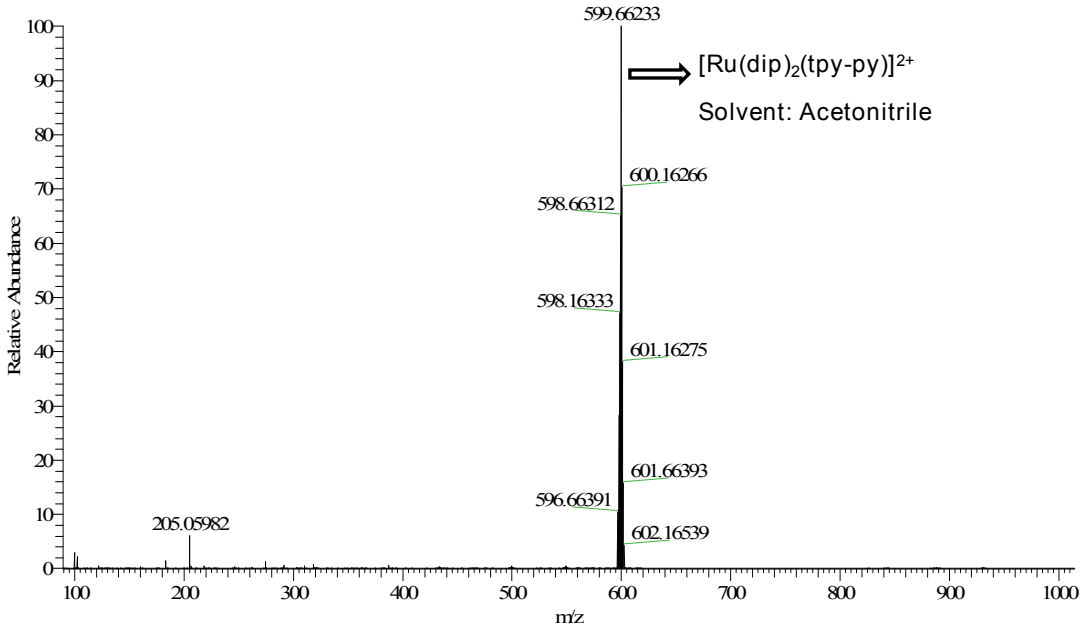

Fig. S5 ESI mass spectrum of complex **1 (**calculated m/z for M^{2+}: 599.6625, found: 599.6623).

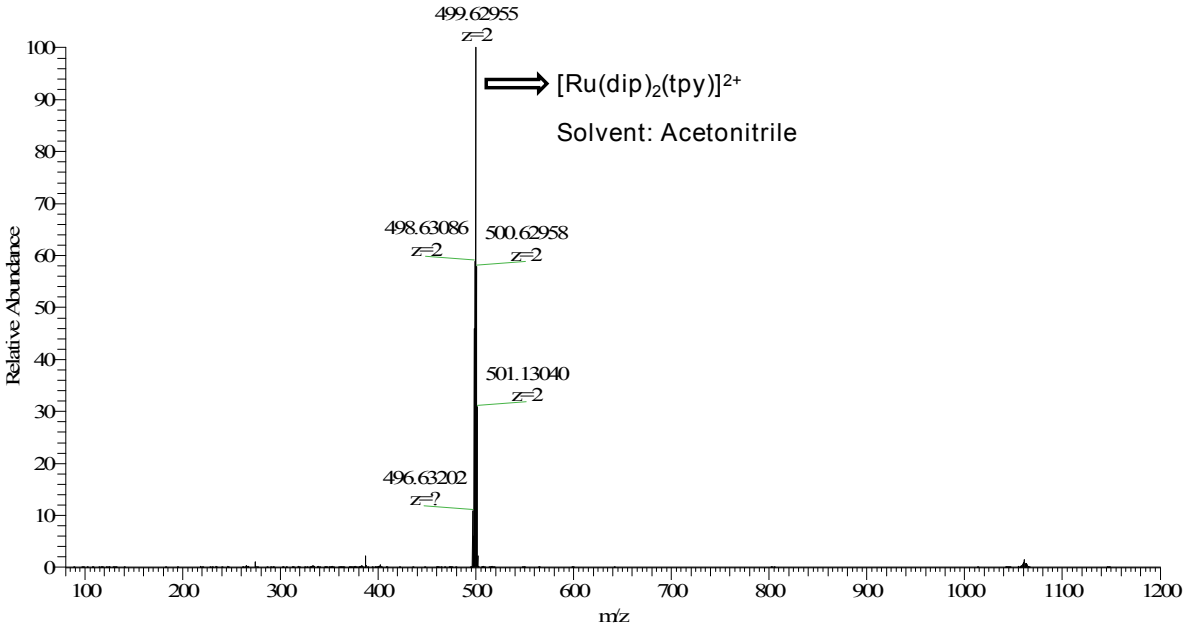

Fig. S6 ESI mass spectrum of complex **2 (**calculated m/z for M^{2+}: 499.6312, found: 499.6296.

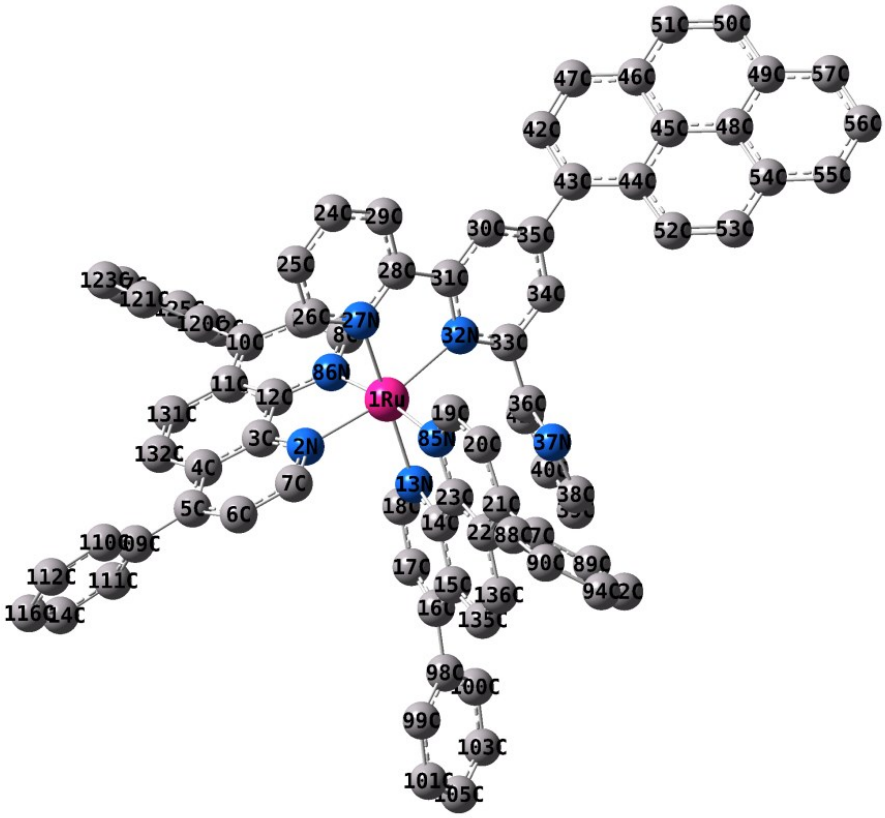

Fig. S7 The optimized structure of complex **1** obtained by Gaussian calculation.

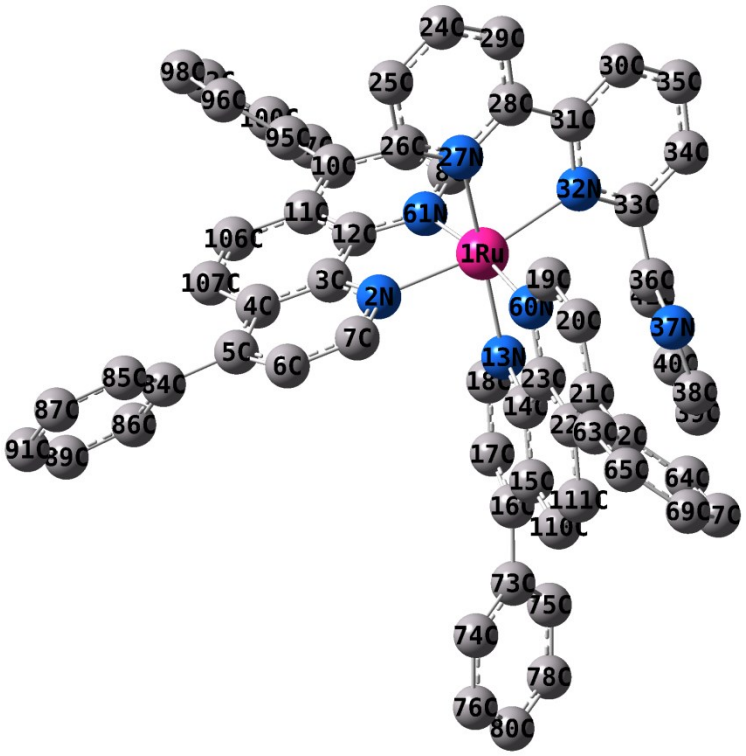

Fig. S8 The optimized structure of complex **2** obtained by Gaussian calculation.

Table S1. Selected bond lengths [Å] of complex **1**[a]

Lengths	
1Ru-32N	2.192
1Ru-27N	2.100
1Ru-85N	2.109
1Ru-13N	2.125
1Ru-2N	2.104
1Ru-86N	2.118

[a] The data in the table were obtained by Gaussian calculations

Table S2. Selected bond lengths [Å] of complex **2**[a]

Lengths	
1Ru-32N	2.194
1Ru-27N	2.100
1Ru-60N	2.107
1Ru-13N	2.124
1Ru-2N	2.104
1Ru-61N	2.119

[a] The data in the table were obtained by Gaussian calculations

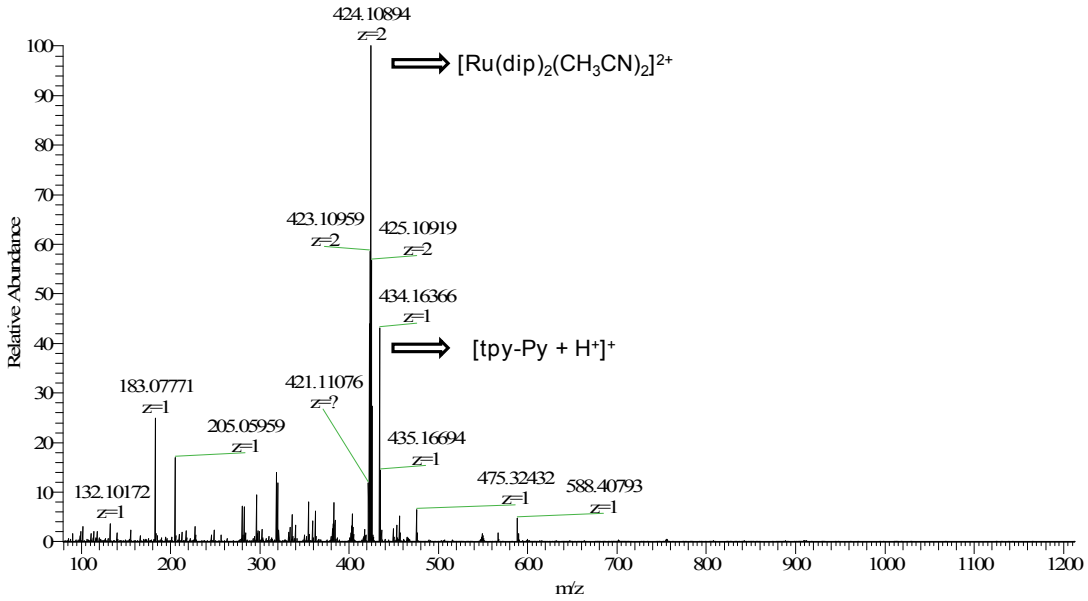

Fig. S9 ESI mass spectrum of complex **1** after irradiation (470 nm, 22.5 mW/cm^2, 30 min) in CH_3CN. The m/z peak at 424.1089 can be ascribed to the compound that tpy-Py ligand was replaced by two CH_3CN. The new peak at 434.1636 is free tpy-Py ligand based.

Calculated m/z for $[Ru(dip)_2(CH_3CN)_2]^{2+}$: 424.1101, found: 424.1089;

Calculated m/z for $[tpy\text{-}Py + H^+]^+$: 434.1657, found: 434.1636.

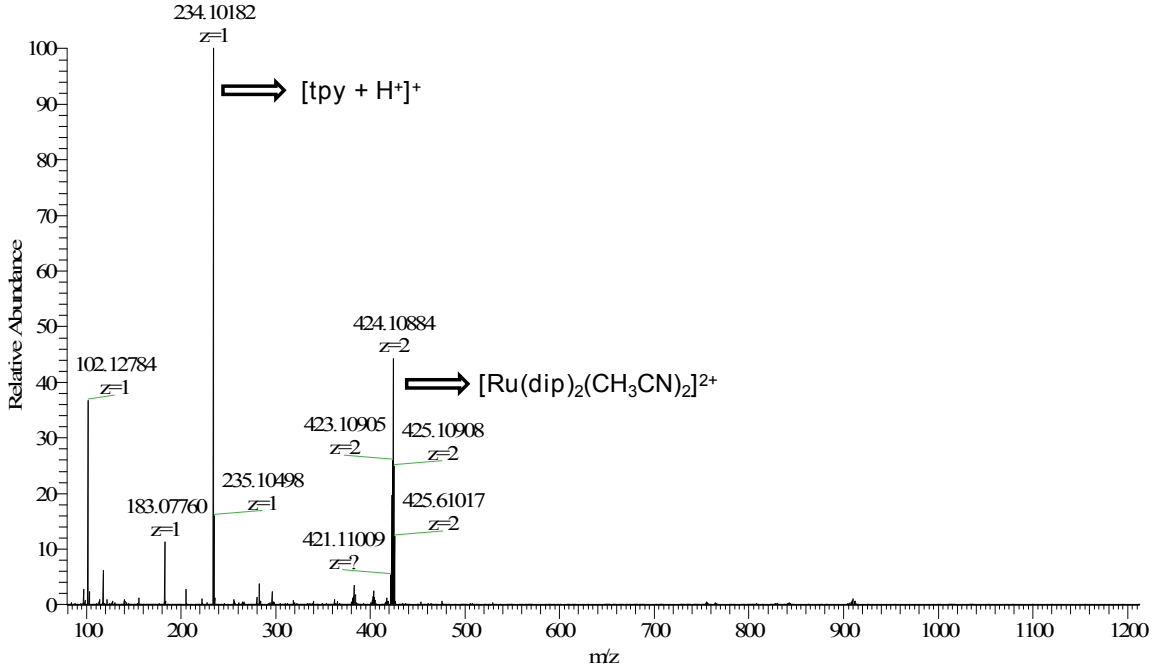

Fig. S10 ESI mass spectrum of complex **2** after irradiation (470 nm, 22.5 mW/cm^2, 30 min) in CH_3CN. The m/z peak at 424.10884 can be ascribed to the compound that the tpy ligand was replaced by two CH_3CN. The peak at 234.1018 is free tpy ligand based.

Calculated m/z for $[Ru(dip)_2(CH_3CN)_2]^{2+}$: 424.1101, found: 424.1088;

Calculated m/z for $[tpy + H^+]^+$: 234.1031, found: 234.1018.

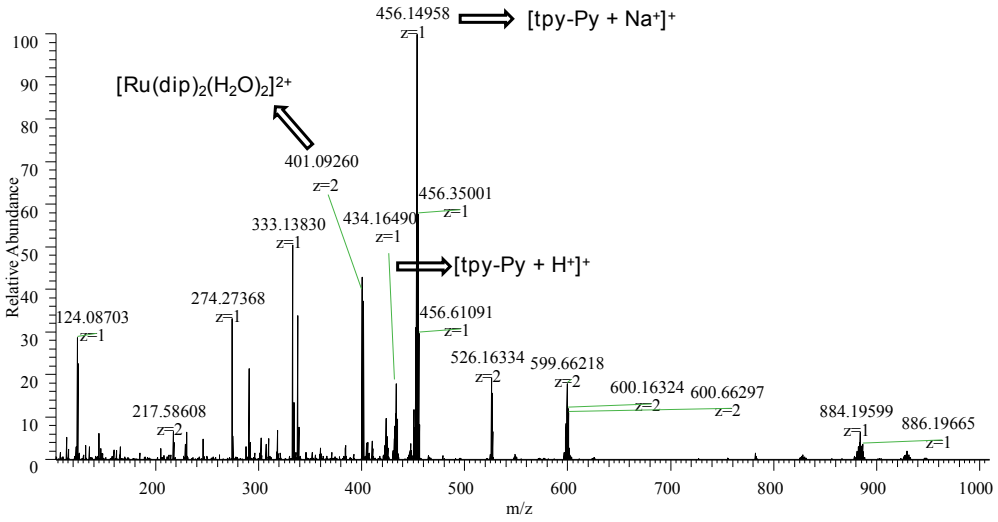

Fig. S11 ESI mass spectrum of complex **1** after irradiation (470 nm, 22.5 mW/cm^2, 30 min) in H_2O. The m/z peak at 401.0926 can be ascribed to the compound that tpy-Py ligand was replaced by two H_2O. The new peak at 434.1649 is free tpy-Py ligand based.

Calculated m/z for $[Ru(dip)_2(H_2O)_2]^{2+}$: 401.0935, found: 401.0926;

Calculated m/z for $[tpy\text{-}Py + Na^+]^+$: 456.1477, found: 456.1496

Calculated m/z for $[tpy\text{-}Py + H^+]^+$: 434.1657, found: 434.1649.

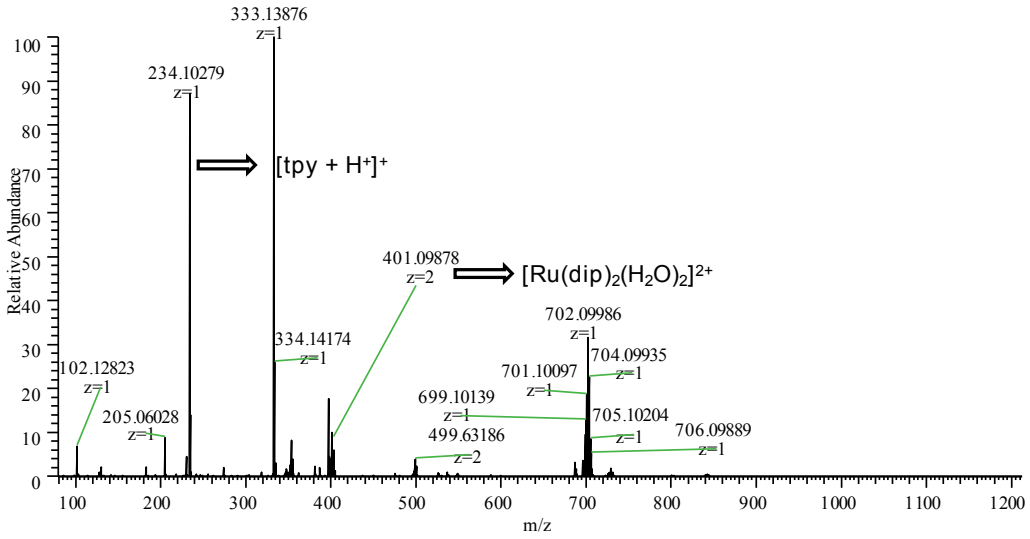

Fig. S12 ESI mass spectrum of complex **2** after irradiation (470 nm, 22.5 mW/cm^2, 30 min) in H_2O. The m/z peak at 401.0920 can be ascribed to the compound that tpy ligand was replaced by two H_2O. The new peak at 234.1028 is free tpy ligand based.

Calculated m/z for $[Ru(dip)_2(H_2O)_2]^{2+}$: 401.0935, found: 401.0988;

Calculated m/z for $[tpy + H^+]^+$: 234.1031, found: 234.1028.

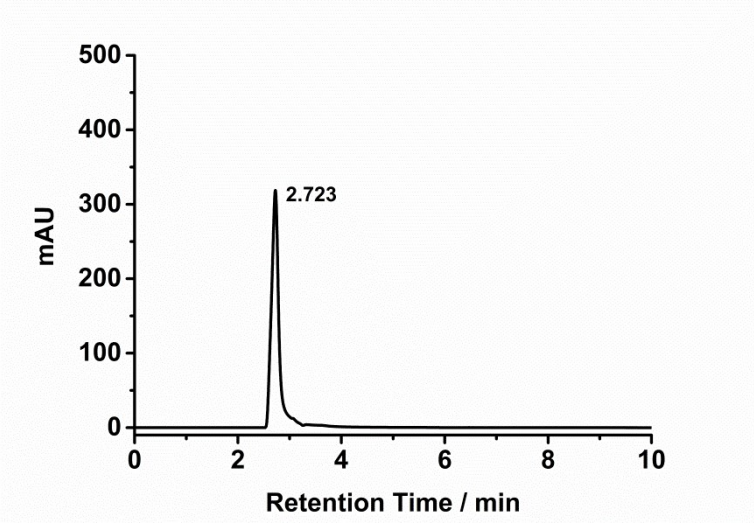

Fig. S13 HPLC chromatogram of **1**. Acetonitrile/water: 95/5 (v/v, containing 0.3% formic acid); flow rate: 0.1 mL/min; detection at 360 nm.

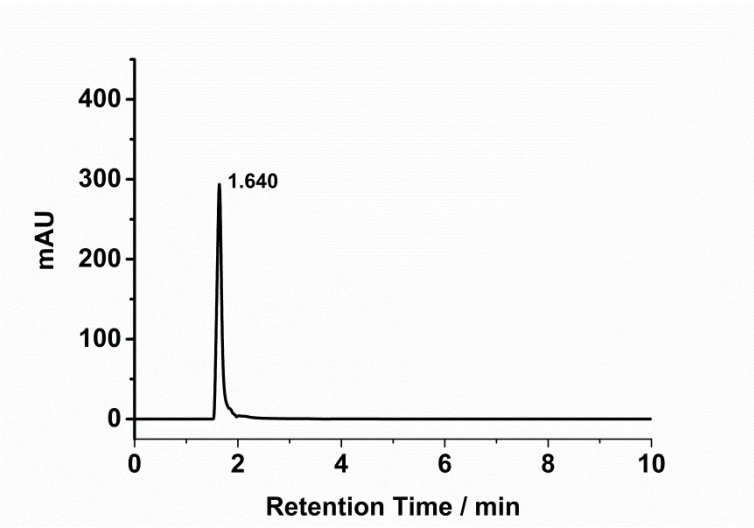

Fig. S14 HPLC chromatogram of **2.** Acetonitrile/water: 97/3 (v/v, containing 0.1% formic acid); flow rate: 0.1 mL/min; detection at 360 nm.

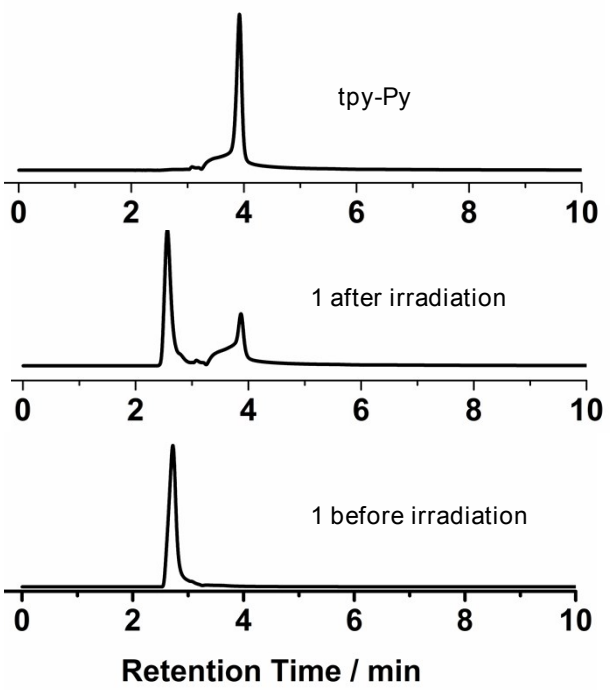

Fig. S15 HPLC chromatogram of ligand tpy-Py (top), complex **1** before (bottom) and after (middle) irradiation (470 nm, 22.5 mW/cm^2, 30 min) in CH_3CN. Acetonitrile/water: 95/5 (v/v, containing 0.3% formic acid); flow rate: 0.1 mL/min; detection at 360 nm.

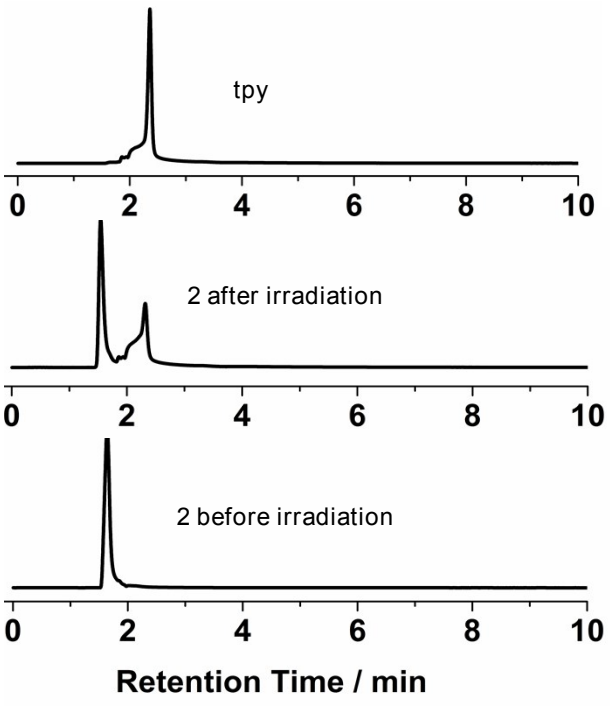

Fig. S16 HPLC chromatogram of ligand tpy (top), complex **2** before (bottom) and after (middle) irradiation (470 nm, 22.5 mW/cm^2, 30 min) in CH_3CN. Acetonitrile/water: 97/3 (v/v, containing 0.1% formic acid); flow rate: 0.1 mL/min; detection at 360 nm.

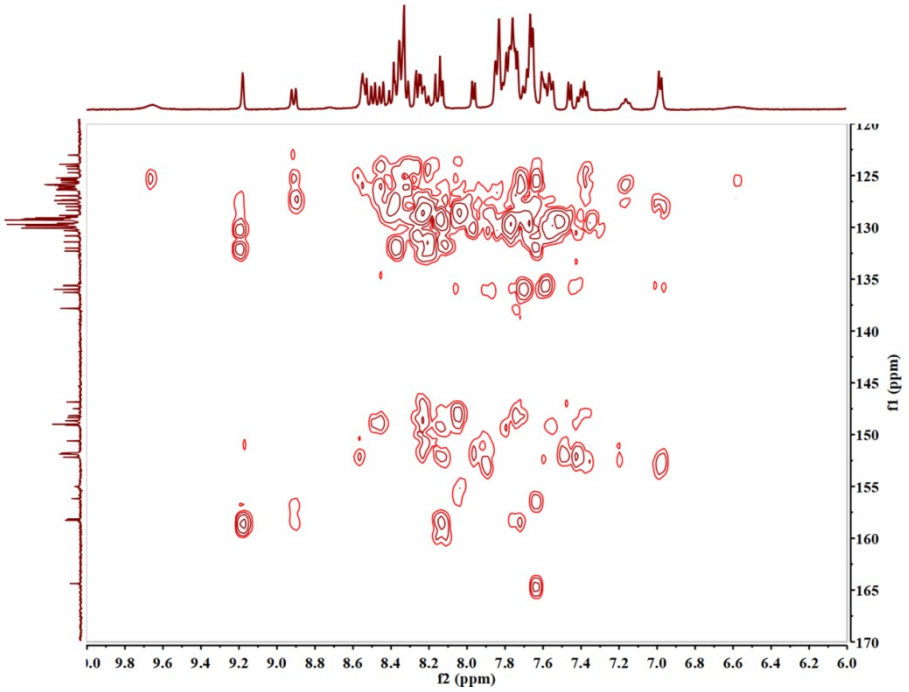

Fig. S17 ^{1}H-^{13}C 2D NMR spectrum of complex **1** in CD_3CN.

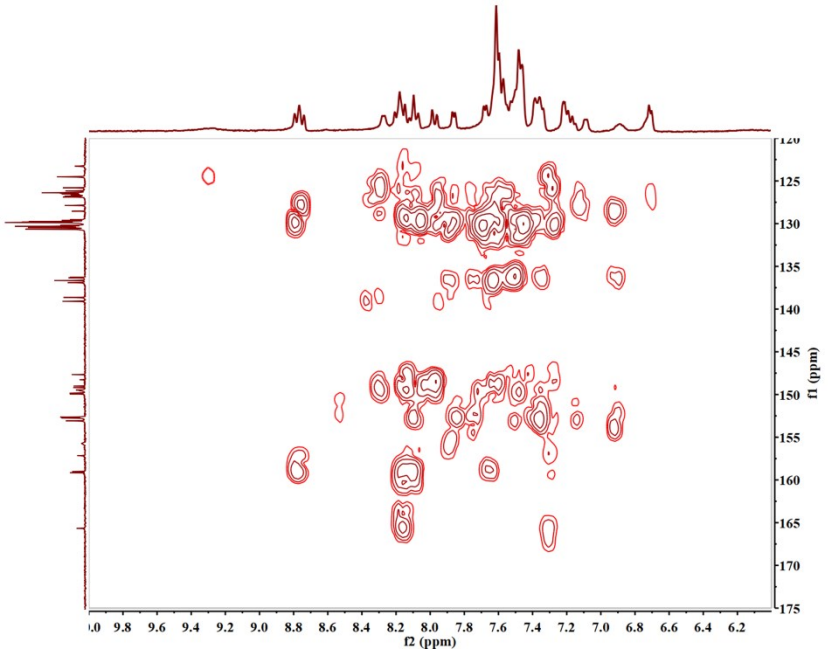

Fig. S18 ^{1}H-^{13}C 2D NMR spectrum of complex **2** in CD_3CN.

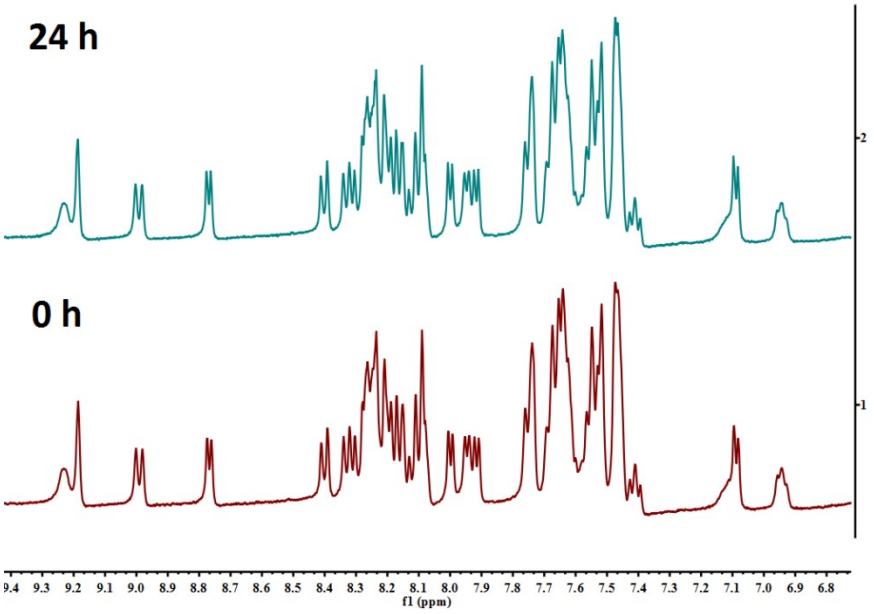

Fig. S19 ^{1}H NMR spectra changes of complex **1** in CD_3COCD_3/D_2O = 2:1 in the dark.

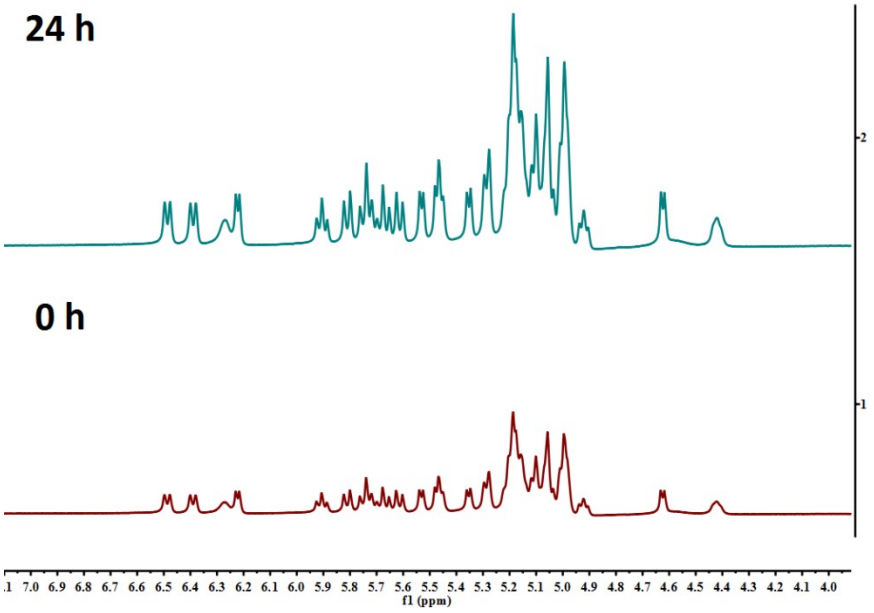

Fig. S20 ^{1}H NMR spectra changes of complex **2** in CD_3COCD_3/D_2O = 2:1 in the dark.

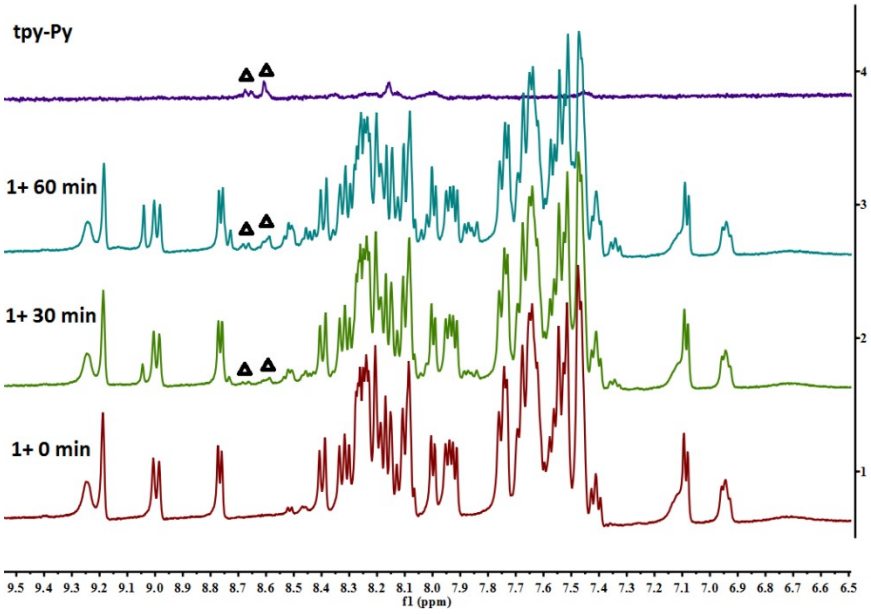

Fig. S21 ^{1}H NMR spectra changes of complex **1** in CD_3COCD_3/D_2O = 2:1 as a function of irradiation (470 nm, 22.5 mW/cm^2) times. The spectrum of free tpy-Py ligand was also provided for comparison. ∆ represents the free tpy-Py ligand.

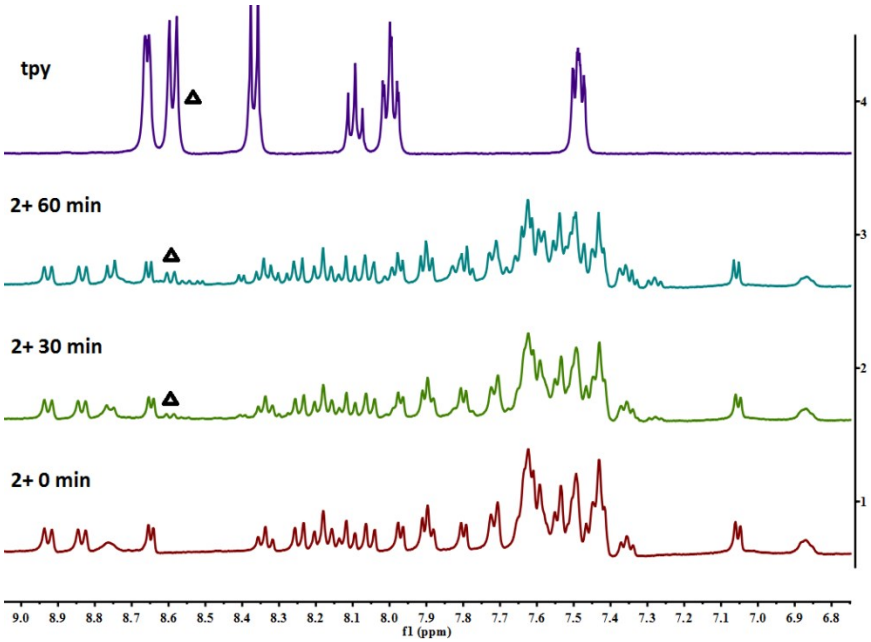

Fig. S22 ^{1}H NMR spectra changes of complex **2** in CD_3COCD_3/D_2O = 2:1 as a function of irradiation (470 nm, 22.5 mW/cm^2) times. The spectrum of free tpy ligand was also provided for comparison. ∆ represents the free tpy ligand.

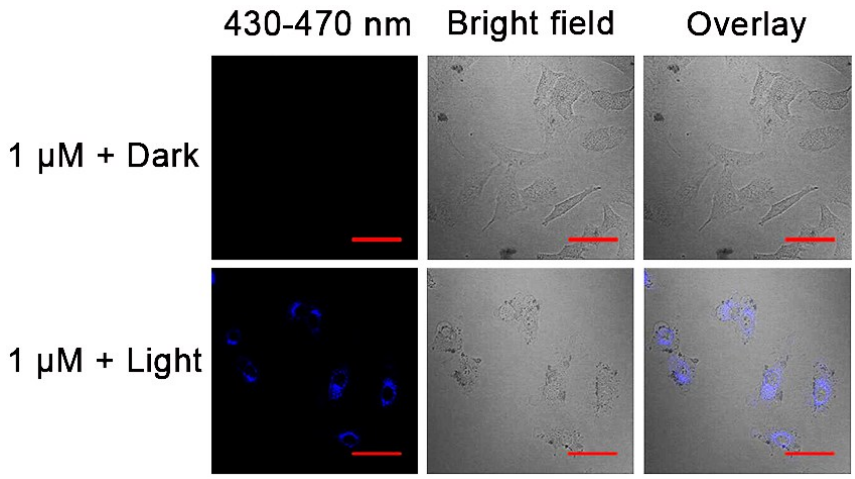

Fig. S23 Confocal imaging of complex **1** in A549 cells before (top) and after illumination (bottom, 470 nm, 22.5 mW/cm^2, 5 min). The blue fluorescence can be ascribed to the photo-released tpy-Py based. Scale bars: 50 μm.

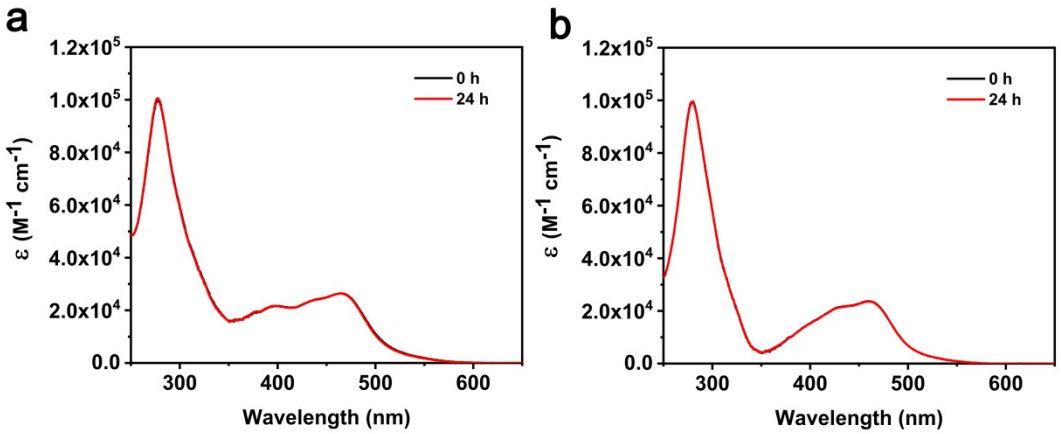

Fig. S24 Absorption spectra changes of **1** and **2** (10 μM) in H_2O (pH=7.0) after 24 h in the dark.

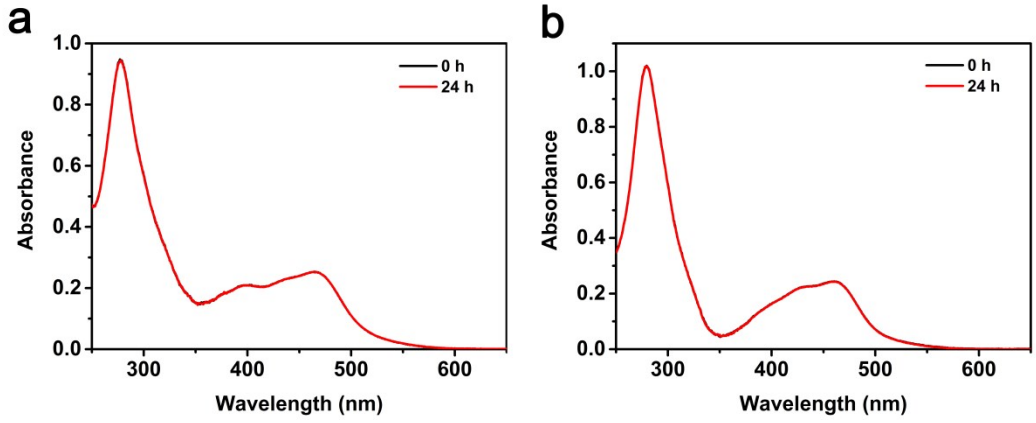

Fig. S25 Absorption spectra changes of **1** and **2** (10 μM) in H_2O (pH=5.5) for 24 h in the dark.

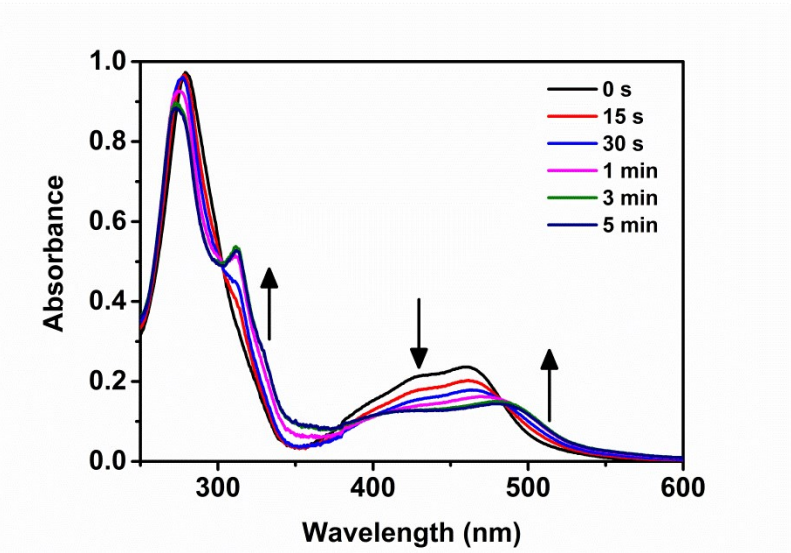

Fig. S26 Absorption spectra changes of complex **2** (10 μM) in H_2O upon LED irradiation (470 nm, 22.5 mW/cm^2).

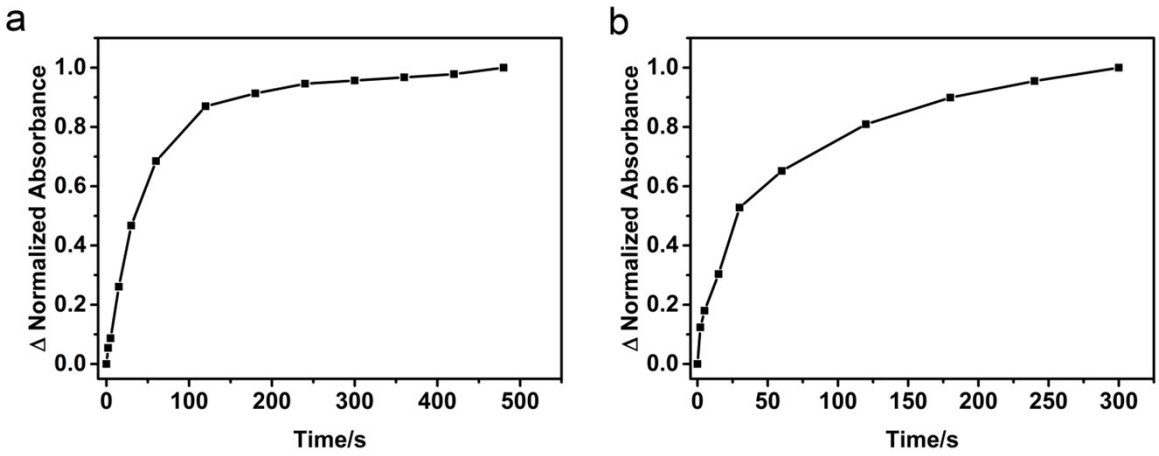

Fig. S27 Normalized absorption changes of **1** (a) and **2** (b) at 510 nm as a function of irradiation time.

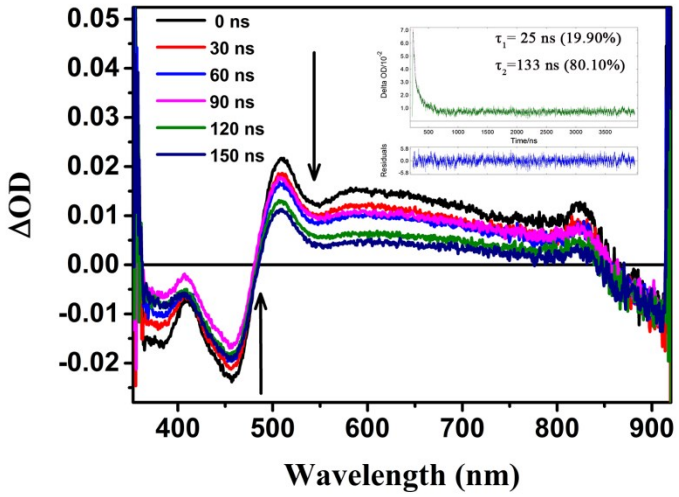

Fig. S28 Transient absorption spectra of complex **1** in degassed CH_3CN upon excitation at 450 nm by a pulsed laser. Inset is the transient absorption decay at 510 nm.

Table S3. Oil(*n*-octanol)-water partition coefficient, singlet oxygen quantum yield and relative ligand dissociation quantum yield of **1** and **2**

Complex	Φ ($^1O_2$) [a]	Log $P_{(Ao/Aw)}$	Φ [b]
1	0.178	2.74	0.46
2	0.019	0.52	1

[a] In CH_3OH

[b] Relative quantum yield of photo-induced ligand dissociation (in H_2O, λ_{irr} = 470 nm)

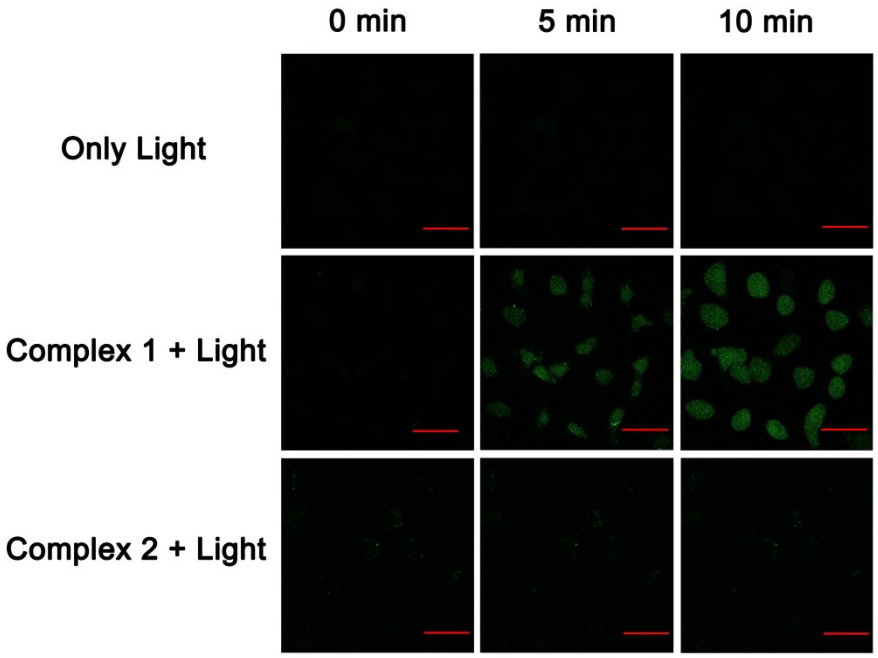

Fig. S29 Confocal microscope images of A549 intracellular $^1O_2$ production by complexes **1** and **2** (0.5 μM) upon one-photon (488 nm, 50 mW/cm^2) irradiation for 0 min, 5 min and 10 min, respectively. DCFH-DA was used as the intracellular ROS probe. λ_{ex}: 488 nm; λ_{em}: 480-520 nm (DCF). Scale bars: 50 μm.

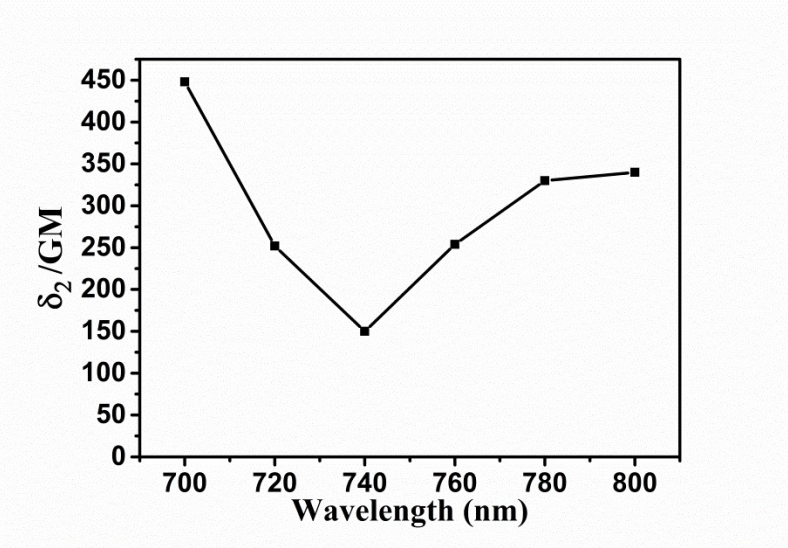

Fig. S30 δ_2 values of tpy-Py within 700-800 nm.

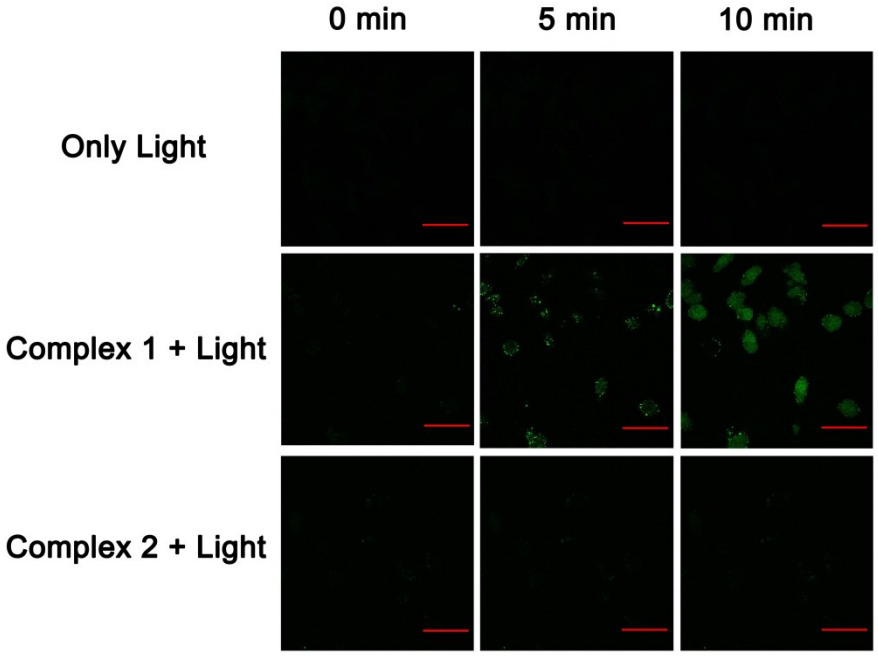

Fig. S31 Confocal microscope images of A549 intracellular $^1O_2$ production by complexes **1** and **2** (0.5 μM) upon two-photon (740 nm, 1 W/cm^2) irradiation for 0 min, 5 min and 10 min, respectively. DCFH-DA was used as the intracellular ROS probe. λ_{ex}: 488 nm; λ_{em}: 480-520 nm (DCF). Scale bars: 50 μm.

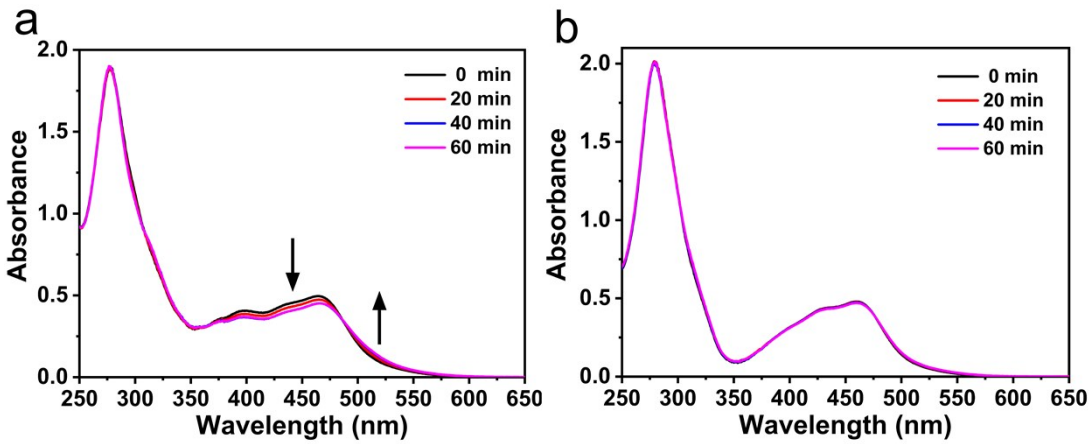

Fig. S32 Absorption spectra changes of complex **1** and **2** (20 μM) in H_2O upon two-photon femtosecond laser (800 nm, 1 W/cm^2) irradiation.

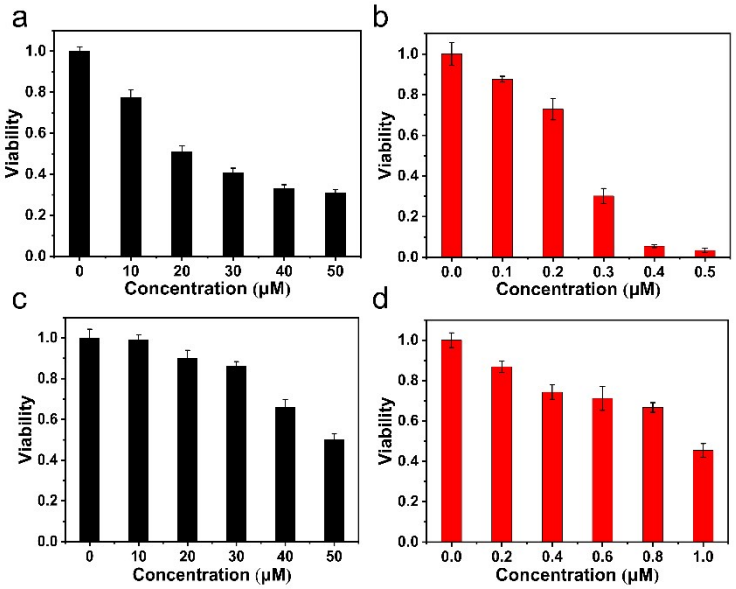

Fig. S33 Cytotoxicity of complexes **1** (a, b) and **2** (c, d) towards A549 cells in the dark (a, c) or upon irradiation (b, d) with a 470 nm LED lamp for 30 min (22.5 mW/cm^2).

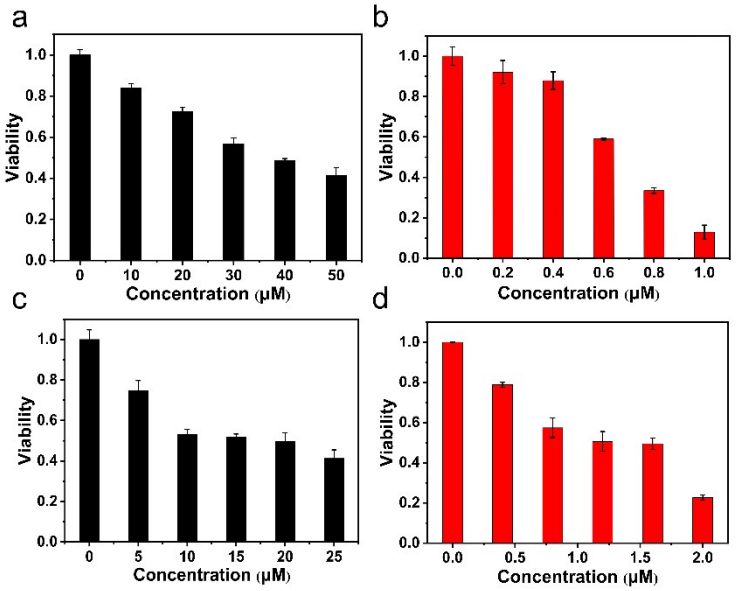

Fig. S34 Cytotoxicity of complexes **1** (a, b) and **2** (c, d) towards HeLa cells in the dark (a, c) or upon irradiation (b, d) with a 470 nm LED lamp for 30 min (22.5 mW/cm^2).

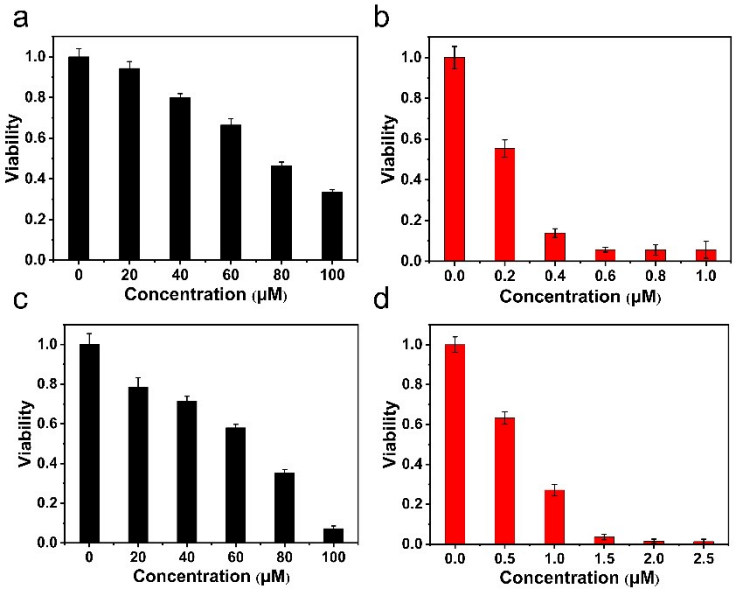

Fig. S35 Cytotoxicity of complexes **1** (a, b) and **2** (c, d) towards A549/Cis cells in the dark (a, c) or upon irradiation (b, d) with a 470 nm LED lamp for 30 min (22.5 mW/cm^2).

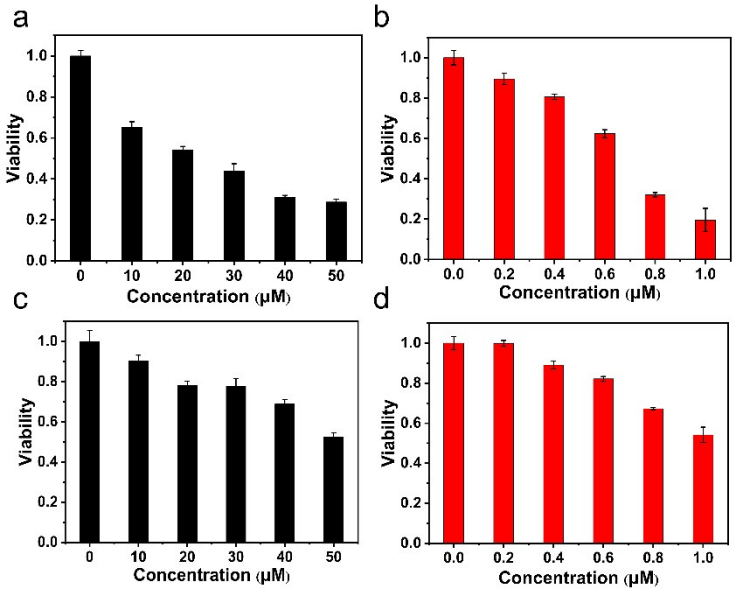

Fig. S36 Cytotoxicity of complexes **1** (a, b) and **2** (c, d) towards A549 cells under hypoxic conditions (3% O_2) in the dark (a, c) or upon irradiation (b, d) with a 470 nm LED lamp for 30 min (22.5 mW/cm^2).

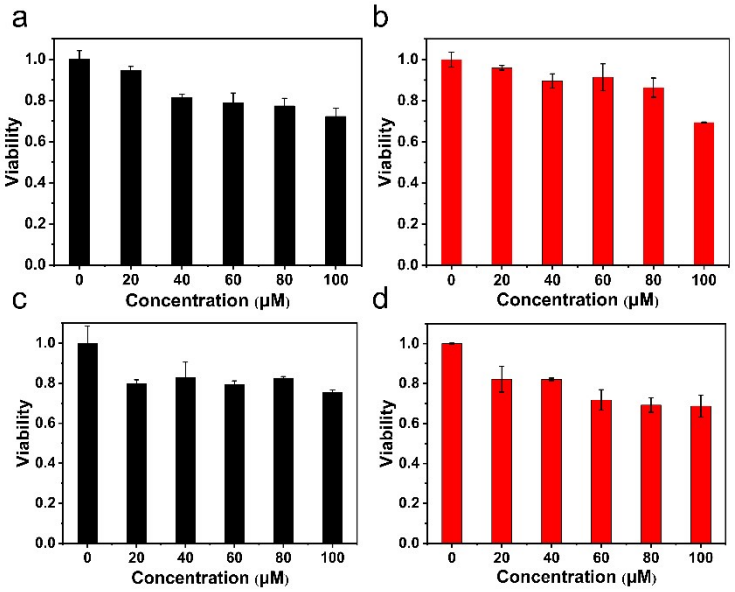

Fig. S37 Cytotoxicity of **Cisplatin** towards A549 (a, b) and A549/Cis (c, d) cells in the dark (a, c) or upon irradiation (b, d) with a 470 nm LED lamp for 30 min (22.5 mW/cm^2).

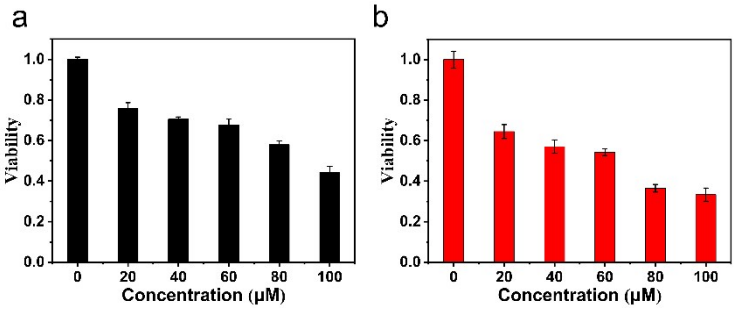

Fig. S38 Cytotoxicity of **tpy-Py** towards A549 (a, b) cells in the dark (a) or upon irradiation (b) with a 470 nm LED lamp for 30 min (22.5 mW/cm^2).

Table S4 IC_{50} values (μM) of **1** and **2** towards various cancer cells

	A549 (Normoxia)		PI[b]	HeLa (Normoxia)		PI[b]	A549 (Hypoxia, 3% O_2)		PI[b]	A549/Cis		PI[b]
	Dark	Light[a]		Dark	Light[a]		Dark	Light[a]		Dark	Light[a]	
1	20 ± 3	0.26 ± 0.01	76	36 ± 4	0.74 ± 0.06	49	21.89 ± 0.90	0.67 ± 0.02	33	60 ± 3	0.21 ± 0.01	285
2	49 ± 4	0.96 ± 0.07	51	9.34 ± 0.87	1.42 ± 0.08	7	50 ± 3	1.04 ± 0.05	48	64.50 ± 0.87	0.64 ± 0.03	101
Cisplatin	> 100	> 100			-[c]			-	-	> 100	> 100	-

[a] Upon irradiation with a 470 nm LED lamp (22.5 mW/cm^2) for 30 min; [b] PI (phototoxicity index) = $IC_{50}^{dark}/IC_{50}^{light}$; [c] – means not measured.

Table S5 A549 cellular uptake levels of complexes **1-2**.

pmol/10^6cell [a]	Nucleus	Cytoplasm	Total
1	15 ± 5	288 ± 30	302 ± 26
2	3.46 ± 0.05	49 ± 3	52 ± 3

[a] Measured by Ru content using inductively coupled plasma mass spectrometry (ICP-MS)

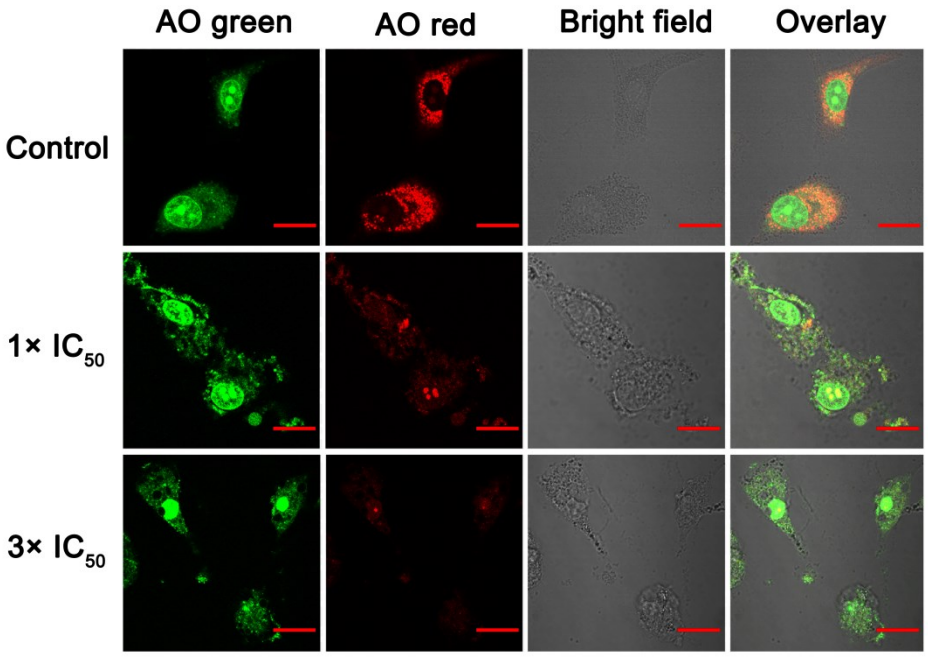

Fig. S39 Lysosomal damage of A549 cells by complex **2** determined by confocal microscopy (AO green fluorescence: λ_{ex} = 488 nm and λ_{em} = 510 ± 20 nm; AO red fluorescence: λ_{ex} = 488 nm and λ_{em} = 625 ± 20 nm). Scale bars: 20 μm.

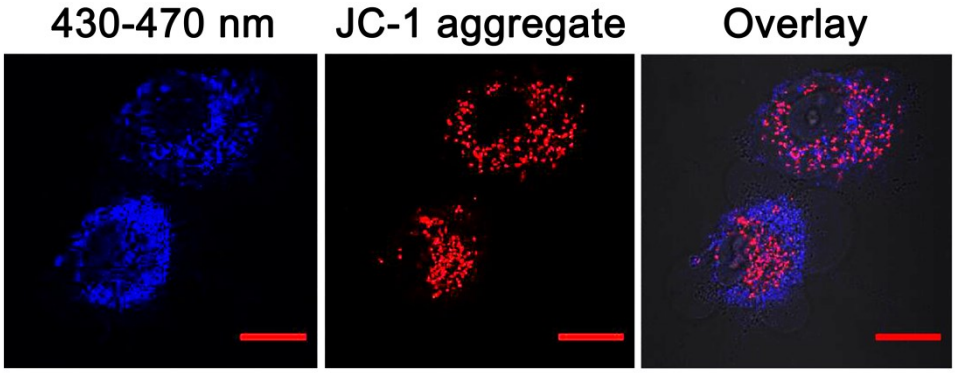

Fig. S40 Confocal colocalization imaging of complex **1** in A549 cells upon illumination (left, 470 nm, 22.5 mW/cm^2, 5 min) and mitochondria stained by JC-1. Scale bars: 20 μm.

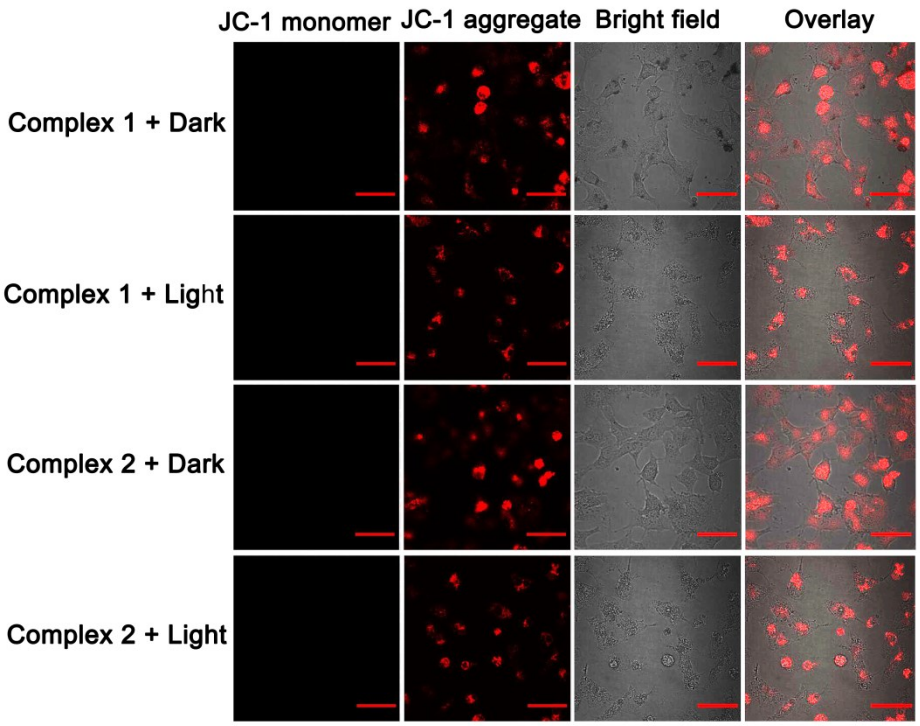

Fig. S41 Detection of mitochondrial membrane potential by JC-1 staining. Scale bars: 50 μm.

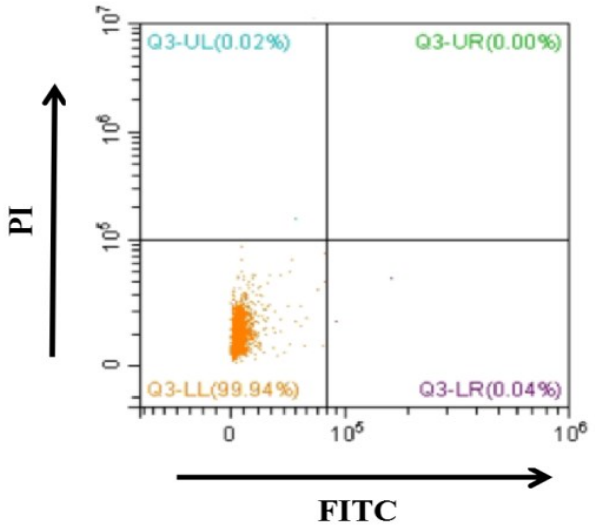

Fig. S42 Flow-cytometric analysis of A549 cells based on Annexin V-FITC and PI staining. The cells were treated with only 470 nm light for 30 min (22.5 mW/cm^2).

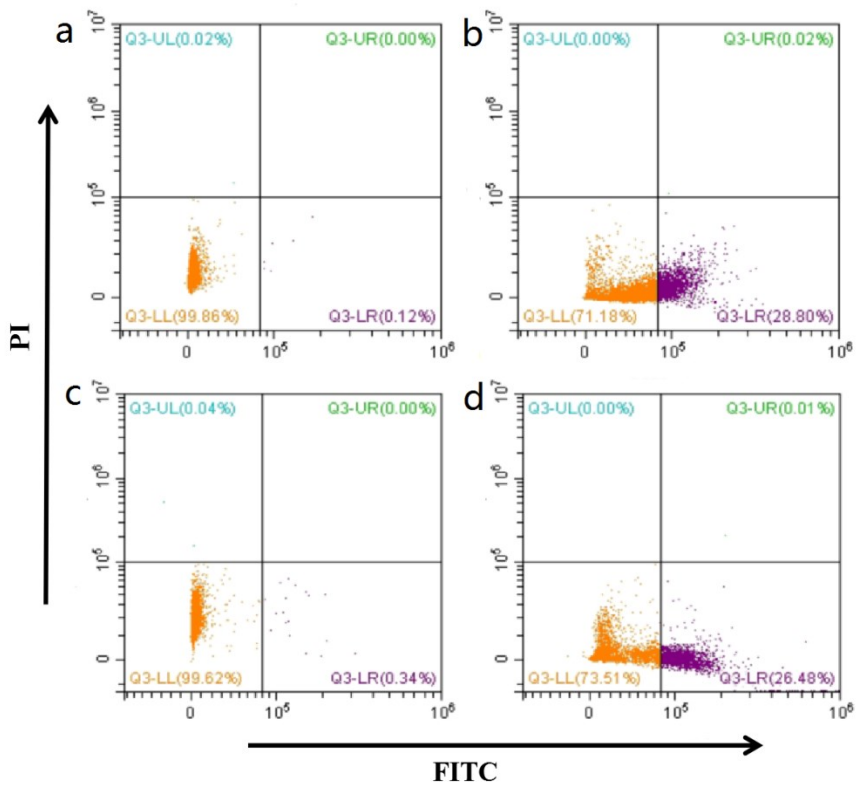

Fig. S43 Flow-cytometric analysis of A549 cells based on Annexin V-FITC and PI staining. The cells were treated with complex **1** (0.5 μM, a and b) or complex **2** (1 μM, c and d) in the dark (a, c), or with irradiation for 30 min (b, d) (470 nm, 22.5 mW/cm^2).

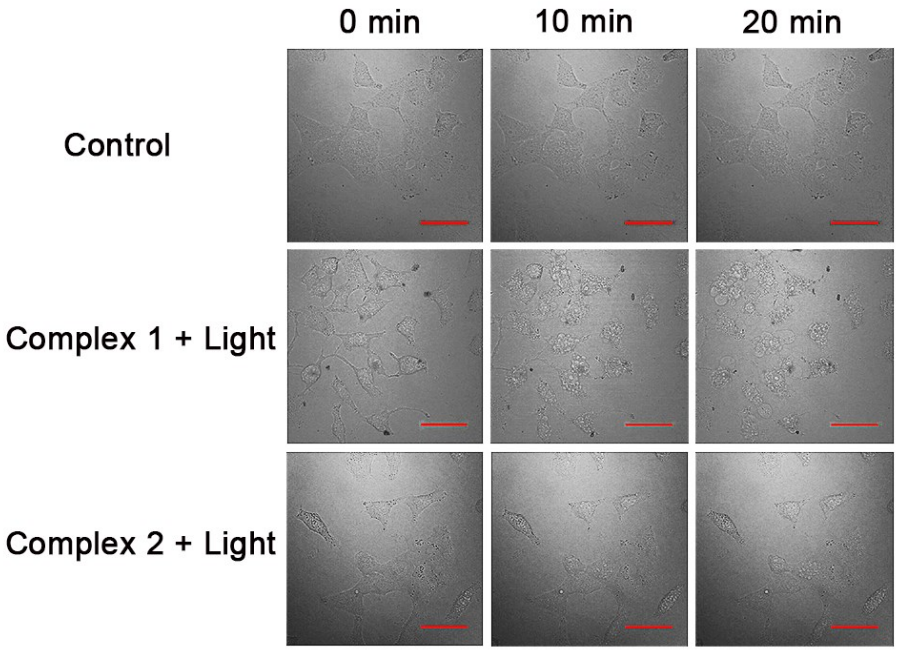

Fig. S44 Confocal images of A549 cells treated only with femtosecond laser irradiation (740 nm, 1.9 W/cm^2) and treated with complex **1** and **2** (0.5 μM) upon two-photon irradiation (740 nm, 1 W/cm^2) for different times. Scale bars: 50 μm.

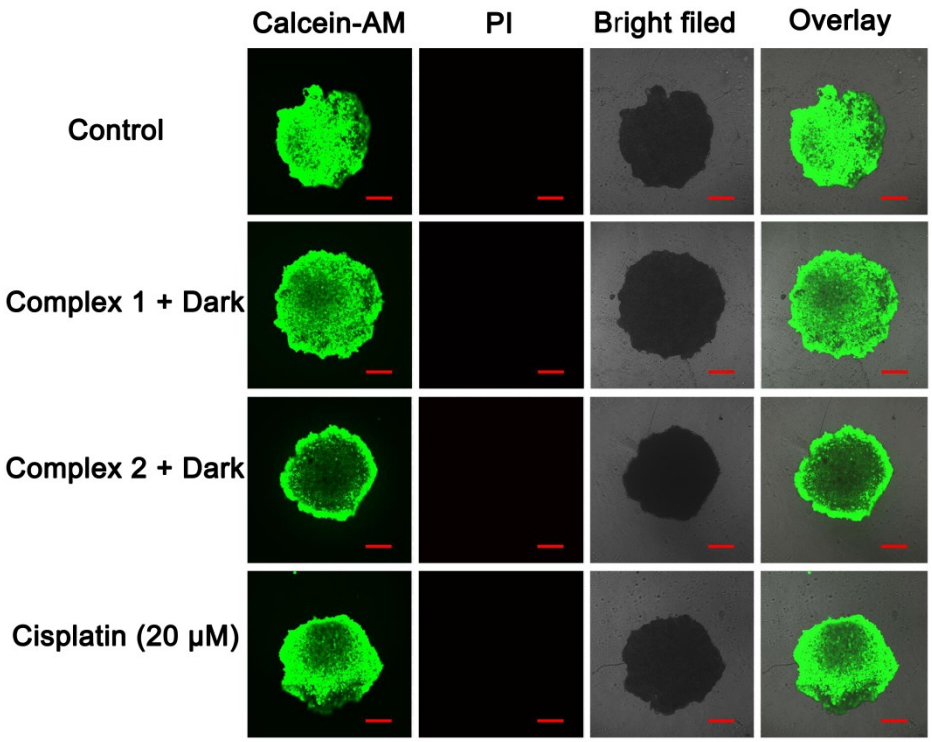

Fig. S45 Images of A549/Cis MCSs treated by **1** or **2** (0.5 μM) without two-photon irradiation and stained by Calcein-AM (λ_{ex} = 495 nm, λ_{em} = 515 nm) and PI (λ_{ex} = 535 nm, λ_{em} = 617 nm). Cisplatin without irradiation was studied. Scale bars: 200 μm.

References

S1. M. J. Frisch, G. W. Trucks, H. B. Schlegel, G. E. Scuseria, M. A. Robb, J. R. Cheeseman, G. Scalmani, V. Barone, B. Mennucci, G. A. Petersson, H. Nakatsuji, M. Caricato, X. Li, H. P. Hratchian, A. F. Izmaylov, J. Bloino, G. Zheng, J. L. Sonnenberg, M. Hada, M. Ehara, K. Toyota, R. Fukuda, J. Hasegawa, M. Ishida, T. Nakajima, Y. Honda, O. Kitao, H. Nakai, T. Vreven, J. A. Montgomery, Jr., J. E. Peralta, F. Ogliaro, M. Bearpark, J. J. Heyd, E. Brothers, K. N. Kudin, V. N. Staroverov, T. Keith, R. Kobayashi, J. Normand, K. Raghavachari, A. Rendell, J. C. Burant, S. S. Iyengar, J. Tomasi, M. Cossi, N. Rega, J. M. Millam, M. Klene, J. E. Knox, J. B. Cross, V. Bakken, C. Adamo, J. Jaramillo, R. Gomperts, R. E. Stratmann, O. Yazyev, A. J. Austin, R. Cammi, C. Pomelli, J. W. Ochterski, R. L. Martin, K. Morokuma, V. G. Zakrzewski, G. A. Voth, P. Salvador, J. J. Dannenberg, S. Dapprich, A. D. Daniels, O. Farkas, J. B. Foresman, J. V. Ortiz, J. Cioslowski, and D. J. Fox, Gaussian 09, Gaussian, Inc., Wallingford CT, 2013.

S2. (a) A. D. Becke, *J. Chem. Phys.*,1993, **98**, 5648-5652; (b) C. Lee, W. Yang, R. G. Parr, *Phys Rev B Condens Matter*, 1988, **37**, 785-789.

S3. P. J. H. a. R. L. M. L. E. Roy, *J. Chem. Theory Comput.*, 2008, **4**, 1029-1031.

S4. (a) W. M. M. Francl, W. J. H. J. Pietro, J. S. Binkley, M. S. Gordon, D. J. Defrees and J. A. Pople, *J. Chem. Phys.*, 1982, **77**, 3654-3665; (b) P. C. Hariharan and J. A. Pople, *Theor. Chim. Acta.*, 1973, **28**, 213-222.

S5. P. D. B. Ayman A. Abdel-Shafi, Roger J. Mortimer, and Francis Wilkinson, *J. Phys. Chem.*, 2000, **104**, 192-202.

S6. R. Joseph, A. Nkrumah, R. J. Clark, E. Masson, *J. Am. Chem. Soc.*, 2014, **136**, 6602-6607.
S7. Q. X. Zhou, W. H. Lei, X. S. Wang and B. W. Zhang, *Inorg. Chem.*, 2010, **49**, 4729-4731.